

# IRMOS: The near-InfraRed Multi-Object Spectrograph for the TMT

Stephen Eikenberry<sup>\*a</sup>, David Andersen<sup>b</sup>, Rafael Guzman<sup>a</sup>,  
John Bally<sup>c</sup>, Salvador Cuevas<sup>d</sup>, Murray Fletcher<sup>b</sup>, Rusty Gardhouse<sup>b</sup>, Don Gavel<sup>e</sup>, Anthony  
Gonzalez<sup>a</sup>, Nicolas Gruel<sup>a</sup>, Fred Hamann<sup>a</sup>, Sam Hamner<sup>a</sup>, Roger Julian<sup>a</sup>, Jeff Julian<sup>a</sup>, David Koo<sup>e</sup>,  
Elizabeth Lada<sup>a</sup>, Brian Leckie<sup>b</sup>, J. Alberto Lopez<sup>d</sup>, Roser Pello<sup>f</sup>, Jorge Perez<sup>a</sup>, William Rambold<sup>a</sup>,  
Carlos Roman<sup>a</sup>, Ata Sarajedini<sup>a</sup>, Jonathan Tan<sup>a</sup>, Kim Venn<sup>g</sup>, Jean-Pierre Veran<sup>b</sup>, John Ziegert<sup>a</sup>

<sup>a</sup>University of Florida, 211 Bryant Space Science Ctr, Gainesville, FL 32611;

<sup>b</sup>Herzberg Institute of Astrophysics, NRC-CNRC, Victoria, BC

<sup>c</sup>University of Colorado, Boulder, CO

<sup>d</sup>Universidad Autonoma Nacional de Mexico, Mexico, DF

<sup>e</sup>University of California at Santa Cruz, Santa Cruz, CA

<sup>f</sup>Laboratoire d'Astrophysique de l'Observatoire Midi-Pyrénées, Toulouse, France

<sup>g</sup>University of Victoria, Victoria BC

## ABSTRACT

We present an overview of the near-InfraRed Multi-Object Spectrograph (IRMOS) for the Thirty Meter Telescope, as developed under a Feasibility Study at the University of Florida and Herzberg Institute of Astrophysics. IRMOS incorporates a multi-object adaptive optics correction capability over a 5-arcminute field of regard on TMT. Up to 20 independently-selectable target fields-of-view with  $\sim 2$ -arcsec diameter can be accessed within this field simultaneously. IRMOS provides near-diffraction-limited integral field spectroscopy over the 0.8-2.5  $\mu\text{m}$  bandpass at  $R \sim 1,000$ -20,000 for each target field. We give a brief summary of the Design Reference science cases for IRMOS. We then present an overview of the IRMOS baseline instrument design.

**Keywords:** infrared, spectroscopy, integral field, adaptive optics, tomography

## 1. INTRODUCTION

IRMOS (near-InfraRed Multi-Object Spectrograph) is one of the premier facility instruments envisioned for the Thirty Meter Telescope (TMT) project ([www.tmt.org](http://www.tmt.org)). This paper presents a status report of the University of Florida (UF) and Herzberg Institute of Astrophysics (HIA) concept for IRMOS, which has recently completed its feasibility study phase. IRMOS is best summarized as a Multi-Object Adaptive Optics (MOAO)-fed multi-object integral-field near-infrared spectrograph for the TMT. IRMOS has two basic operational systems within the instrument – an MOAO system for adaptive correction, and a “science backend” for target selection and integral field spectroscopy. The combination of the collecting area of TMT, the unique image-sharpening capabilities of the IRMOS MOAO system, and the multi-integral-field spectra provided by the IRMOS back-end make its capabilities unparalleled for addressing some of the leading scientific challenges of the coming decades. The TMT Science Requirements Document identifies two key science cases for IRMOS – the properties of very high-redshift galaxies ( $z > 5$ ), and the properties of galaxies during the era of peak star formation ( $z \sim 2$ -3). These are among the key science drivers for TMT as a whole, and for Extremely Large Telescopes in general, and motivated the TMT Science Advisory Committee to rank IRMOS as a tie for the top science priority in the instrument suite.

In the sections below, we present an overview of the UF/HIA IRMOS concept. In Section 2, we present a brief summary of the science drivers for IRMOS and the top-level science requirements for the instrument. In Section 3, we present an overview of the baseline IRMOS instrument design.

## 2. IRMOS SCIENCE CASES

As noted above, the TMT Science Requirements Document identifies two key science cases for IRMOS – the properties of very high-redshift galaxies ( $z > 5$ ), and the properties of galaxies during the era of peak star formation ( $z \sim 2-3$ ). These two key cases form the “Design Reference Cases” (DRC) for IRMOS, providing the fundamental performance drivers for the instrument. These same capabilities enable a broad range of additional scientific investigations. In particular, based upon the realization that a DRC-optimized IRMOS can also produce near-diffraction-limited moderate-Strehl images in the H and K-bands, we have developed exciting new cases that exploit this previously-unknown capability. These include investigation of the underlying physics of the bulge/black-hole connection in the Virgo cluster of galaxies and study of the fundamental variations in the stellar initial mass function in the Large Magellanic Cloud.

Due to space constraints, in this paper we simply present a brief summary of the two DRC science cases for IRMOS.

### 2.1 Design Reference Case 1: Properties of Galaxies at the Era of Peak Star Formation

The detailed study of galaxies during the era of peak star formation ( $1 < z < 6$ ) is one of the flagship science drivers for the TMT. This redshift range encompasses no more than the first  $\sim 30\%$  of the age of the Universe, but may account for as much as  $\sim 70\%$  of its total star formation, heavy element production, and black hole accretion. It is also expected that most of the action in assembling massive galaxies likely occurs in this redshift range, making  $1 < z < 6$  the focus of future major galaxy surveys aimed at understanding the physical processes driving galaxy formation and evolution. IRMOS will revolutionize the study of galaxies at this epoch, enabling detailed mapping of their physical properties, including kinematics, metallicity, stellar and gas content, and extinction-corrected star formation rates for thousands of galaxies at  $z = 2-6$ . Such a survey will be a major milestone towards an empirical determination of the physics and timeline of galaxy assembly in this most interesting era of peak star formation activity. (See Figure 1).

### 2.2 Design Reference Case 2: Properties of Galaxies at High Redshift

IRMOS will be the premiere instrument on the TMT for surveying Lyman alpha emitting galaxies at  $z = 6-15$ . The unique capabilities of IRMOS provide the means to probe the star formation history of the universe back to 300 Myrs after the Big Bang and extend observations of galaxy evolution beyond the reionization epoch. The combination of IRMOS and the TMT provide the only efficient means of studying the galaxy population at these redshifts. While the expected surface density of Ly- $\alpha$  emitters remains unconstrained, the flexibility of the IRMOS design enables us to conduct a survey for these galaxies either as the primary science program, or as a piggyback program coupled to other planned observations. A statistical sample that includes 1000 bright Ly- $\alpha$  emitters at  $z > 7.5$  with  $S/N > 10$  per resolution element can be observed in a dedicated twenty night program.

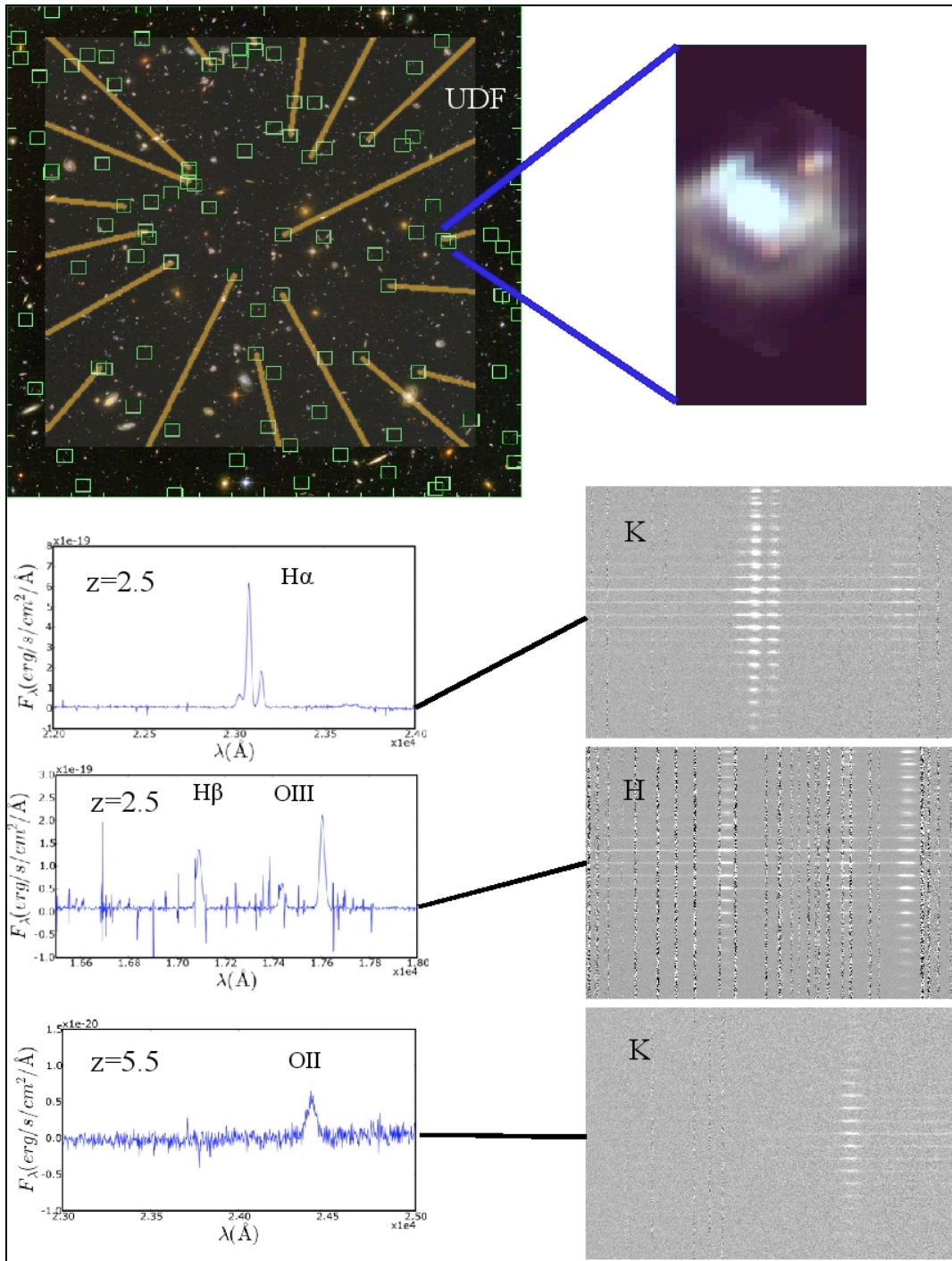


Fig. 1. Simulated IRMOS observations of a typical Lyman-break galaxy at redshifts  $z=2.5$  and  $z=5.5$ . Top right panel: image of the Hubble Ultra Deep Field (UDF). Lyman-break galaxy candidates at  $z=2-6$  are identified with green squares. An actual IRMOS MOS probes configuration is shown in yellow lines. Top left panel: simulated deep near-IR image of a typical Lyman-break galaxy as seen in a single IRMOS IFU. Middle panels: simulated 2-D and 1-D spectra showing characteristic emission lines of Lyman-break galaxies at  $z=2.5$  and  $z=5.5$ .

### 3. IRMOS BASELINE INSTRUMENT OVERVIEW

As noted above, IRMOS is best summarized as a MOAO-fed multi-object integral-field near-infrared spectrograph for the TMT. Its basic parameters are as follows:

Table 1 – IRMOS Basic Parameter Summary

<b>Parameter</b>	<b>Value</b>	<b>Comment</b>
Wavelength	<b>0.8-2.5 <math>\mu\text{m}</math></b>	SRD specification
Spectral resolution	<b>1,000-20,000</b>	Highest resolutions available only at finest pixel scales
Number of MOS probes	<b>20</b>	Driven by balance between target density and cost/size
MOS patrol field	<b>5-arcmin diameter</b>	SRD specification
IFU field of view	<b>2.2-arcsec diameter</b>	Smaller FOV for finer pixel scales
IFU field separation	<b>&lt;1-arcsec min.</b>	Set by probe pickoff size
Slitlet widths	<b>16, 23, 50-milliarcseconds</b>	2-pixel widths matching 50% EED for various cases
Detector format	<b>2048x2048-pix</b>	HAWAII-2RG baseline
Instantaneous Wavelength Coverage	<b>Octave at low resolution; single atmospheric window at R~4,000</b>	
Sensitivity	<b>Sky background limited</b>	Detector noise becomes significant/limiting at higher resolutions

#### 3.1 Basic System Layout

IRMOS has two basic operational systems within the instrument – an MOAO system for adaptive correction (described in more detail in Andersen et al., 2006), and a “science backend” for target selection and integral field spectroscopy. We present a basic block diagram for the IRMOS instrument concept in Figure 2. We have adopted a vertical rotation axis for IRMOS on a large azimuthal bearing, which allows for field derotation of the entire instrument while maintaining a fixed gravity vector for the opto-mechanical systems, thus greatly reducing the impact of differential flexure on IRMOS performance. IRMOS contains two primary vacuum spaces at two different operating temperatures – the “meat locker” and the “deep-freeze” illustrated in the figure. The “meat locker” is a vacuum volume near the TMT input focal plane with an operating temperature of  $\sim 230$  K. It contains parts of the MOAO and all of the MOS (multi-object spectroscopy) subsystems, including pickoff optics and detectors for the various wavefront sensors, the pickoff optics for the science fields, and the deformable mirrors for MOAO correction (which are opto-mechanically integrated into each MOS probe arm). The outputs of the MOS pickoffs of the science field are then directed into separate “deep-freeze” vacuum volumes through a set of small gate valves. This separation allows independent vacuum/thermal control for (and thus access to and maintenance of) the deep-freeze subsystems. The deep-freeze operating temperature is  $\sim 80$  K, and this volume contains the final re-imaging optics for the MOS pickoffs, the integral field units, and the spectrograph optics, mechanisms, and science detectors.

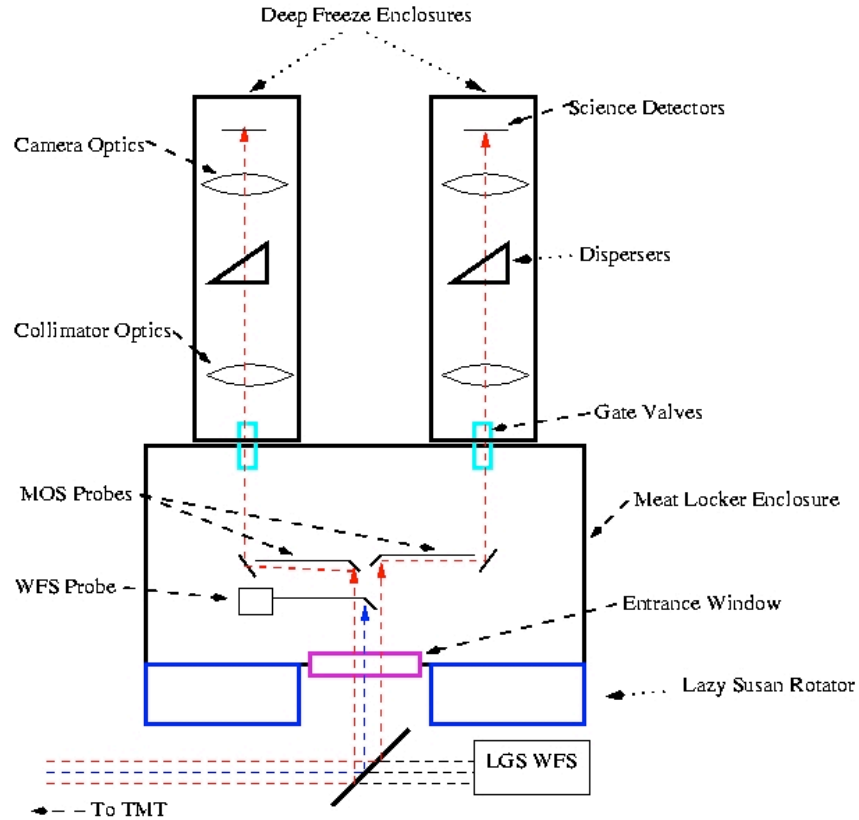


Fig. 2. Concept Schematic for IRMOS. Light enters from the TMT tertiary (to the left) and encounters a dichroic which transmits sodium laser light and reflects longer wavelengths “up” into the “meat locker”.

The MOAO subsystem of IRMOS provides adaptive correction of small ( $\sim 2$ -arcsec) MOS subfields over a much wider ( $\sim 5$ -arcminute) patrol field (or “field of regard” – FOR) at the telescope focal plane. This is accomplished using a combination of LGS (laser guide star) and NGS (natural guide star) WFS (wavefront sensors) over the field. The Atmospheric Dispersion Correctors (ADCs) and MOAO deformable mirrors (DMs) will be opto-mechanically embedded in the MOS subsystem itself, providing integrated AO correction for the science path. The MOS subsystem consists of a set of  $\sim 20$  fixed-optical-path deployable probe arms patrolling the 5-arcminute field-of-regard (FOR). The MOS probes collimate the beam, feed it through several folds, including the MOAO DMs, and then re-image the beam output onto the IRMOS integral field units (IFU). Each IFU accepts the AO-corrected input  $\sim 2$ -arcsec field from a single MOS probe, and then uses image slicer technology to reformat the 2-dimensional field into a pseudo-longslit format with high throughput and a  $>98\%$  fill factor projected onto the sky. Finally, the IFUs feed their AO-corrected sliced fields to a number of moderate-resolution near-IR spectrographs which disperse the light from the pseudo-longslits and capture the final spectrum of each point in the MOS field of view.

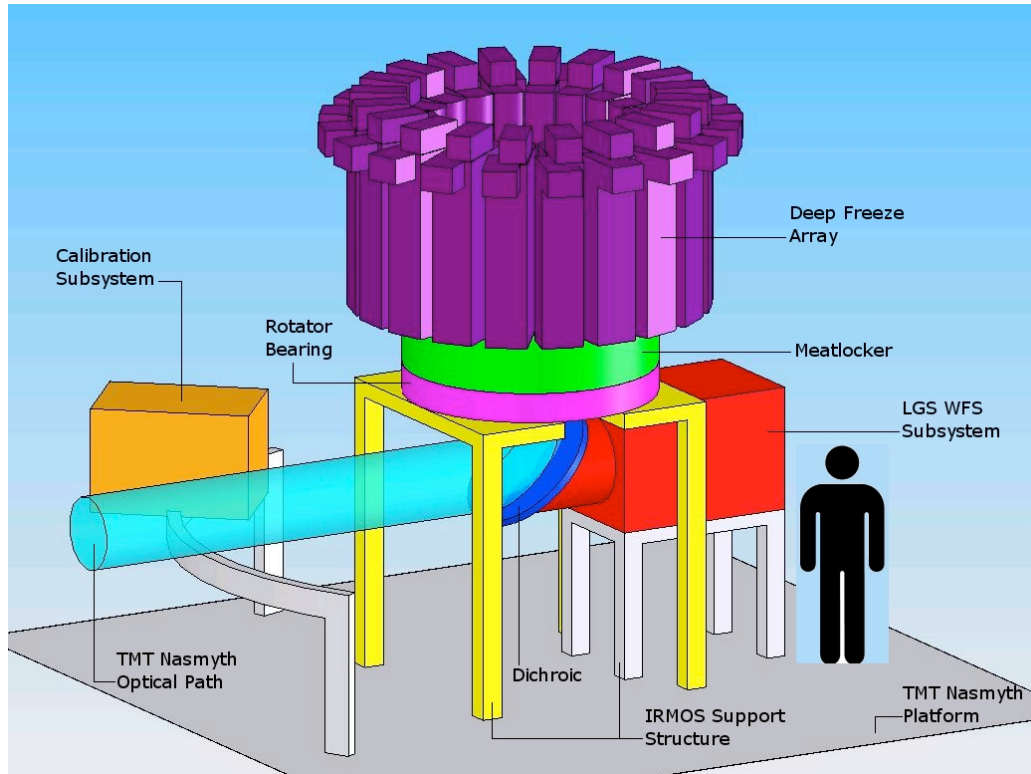


Fig. 3. Scale model of IRMOS on the TMT Nasmyth Platform

### 3.2 Dichroic

The first optical element in IRMOS is a large ( $1.4 \times 1.0 \times 0.2 \text{ m}^3$ ) dichroic that directs light bluewards of 0.6 microns into the LGS WFS subsystem and light redwards of 0.8 microns into the meatlocker subsystem (see Figures 1 and 2). Besides separating the beam, the dichroic also changes the optical axis of the meatlocker and spectrograph subsystems to a vertical orientation; a vertical optical axes allows the instrument to be de-rotated while maintaining a fixed gravitational axis. In principle, the dichroic can direct light up (as in Figure 2) or down depending on the final height of the TMT optical axis above the Nasmyth platform.

### 3.3 LGS WFS Subsystem

IRMOS requires at least 8 LGS to provide adequate tomography over the 5-arcminute patrol FOR. Light bluewards of 0.6 microns passes through the dichroic and enters the LGS subsystem (Figure 4). The LGS subsystem consists of 8 individual “trombone” LGS WFS. The trombone relay consists of 4 flat mirrors, two of which are mounted on a stage and can be translated to adjust the focus of the LGSs. The translation can accommodate changes in the distance to the LGS between 85km to 200km. The WFS itself consists of a lens doublet which collimates the laser light onto a 60x60 Shack-Hartmann (SH) lenslet array and a radial format CCD with 60x60 subarrays of 4x16 pixels and a pixel scale of 0.5 arcseconds.

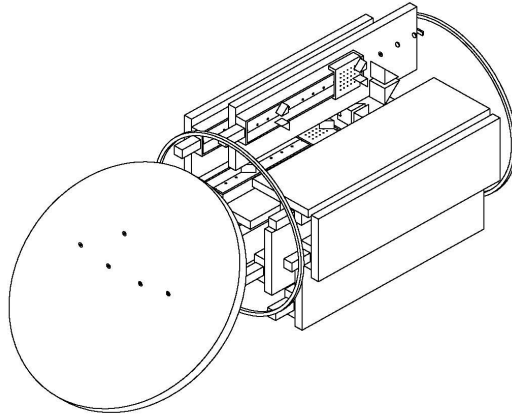


Fig. 4. Laser Guide Star Wavefront Sensor trombone system and dichroic package

### 3.4 Meat Locker Subsystem (NGS WFS and MOS)

The NGS subsystem serves four important purposes: 1) The six probe arms are used for acquisition of the scientific FOV; 2) The multiple arms can be used to measure and control, via feedback to the telescope control system, the telescope-delivered plate scale; 3) Focus measured from the NGS WFS can be used by the real-time control system to track and compensate defocus which would be introduced into science images due to rapid changes in the profile and altitude of the Sodium layer; 4) Finally, but most importantly, the NGS WFS measure the tip-tilt modes of the wavefront which are not measured by the LGS WFS subsystem.

Physically, the NGS WFS subsystem is mounted in the Meat Locker upstream from the telescope focus. It consists of six arms each mounted on a linear and a rotation stage. On each solid arm are all the elements of the WFS. Light from a six arcsecond FOV is picked off at the tip of the arms, and collimated. The pupil will be placed on a 2x2 SH lenselet array which in turn will feed a 128x128 pixel low noise optical EEV CCD60.

The primary function of the MOS probe mechanism is to select target fields-of-view and relay light from them to the IFUs and spectrographs. This is accomplished using 20 independently-controlled/actuated MOS pick-off probe arms. Each arm patrols a sector (“slice of pie”) of the MOAO field, just above the input telescope focal plane (loosely based on the HRNIRS MOS design described in Hinkle et al., 2006; Eikenberry et al., 2006; Muller et al., 2006, Liang et al., 2006). Optics in each arm relay light from a 2-arcsec-diameter field to the IFU corresponding to that arm. The re-imaging optic is selectable among three possible focal lengths, setting the pixel scale for the IFU and spectrograph to 8, 12, or 25-mas per pixel.

Figure 5 shows views of the MOS probe mechanism. The primary structural components of the mechanism are a base plate, to which all probe arm and motor components are mounted, and an outer lid. The lid has a central cutout allowing light in the converging beam from the telescope to fill an unvignetted 5-arcmin-diameter (~655-mm diameter) region at the focal plane. The 20 probe arms each patrol an 18-degree “slice of pie” region just above this focal plane, relaying light to an output focal plane. Inserted into the probe arm optical train are atmospheric dispersion corrector (ADC) prism pairs, as well as the deformable mirrors (DMs) which provide the adaptive correction for the IRMOS MOAO subsystem.

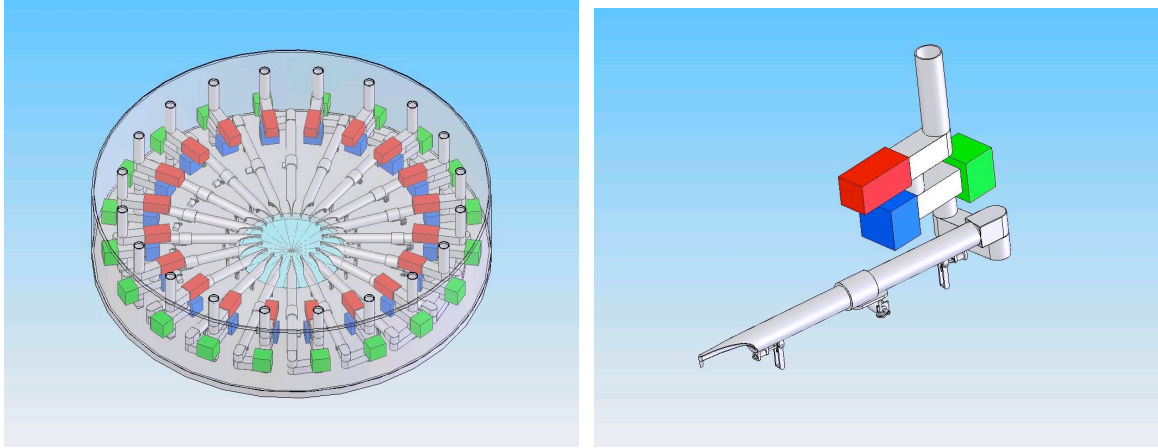


Fig. 5. MOS mechanism. (Left) 20-arm MOS mechanism for IRMOS. (Right) View of a single probe arm, including electronics control boxes for the woofer (blue), tweeter (red), and tip-tilt mirror (green).

The MOAO correction will be introduced by a pair of DMs acting as a “woofer” and “tweeter.” The wavefront error to be corrected by the pair of DMs will first be projected onto the low-order, large stroke woofer DM. The residual wavefront error will then be projected onto the high order, small stroke tweeter DM. The baseline IRMOS design will employ one CILAS 31 actuator bimorph mirror in each arm as the woofer and a 60x60 actuator MEMS mirror. Because the meatlocker will be a vacuum, the tweeter should be a segmented MEMS mirror (segmented mirrors can be mechanically damped in a vacuum, while continuous face sheet MEMS mirrors “ring”).

Figure 4 below shows the MOS probe optical layout in the same orientation as Figure 2. Light enters from the bottom of the figure and comes to a focus at the TMT focal plane. Just above this focal plane, the MOS pickoff mirror sends light down the length of the probe arm, where a doublet lens collimates the beam. The light travels the length of the long arm to the first joint, though the second shorter arm to the second joint. It then encounters a sequence of fold mirrors and MOAO deformable mirrors before exiting out the top of the figure into the deep freeze.



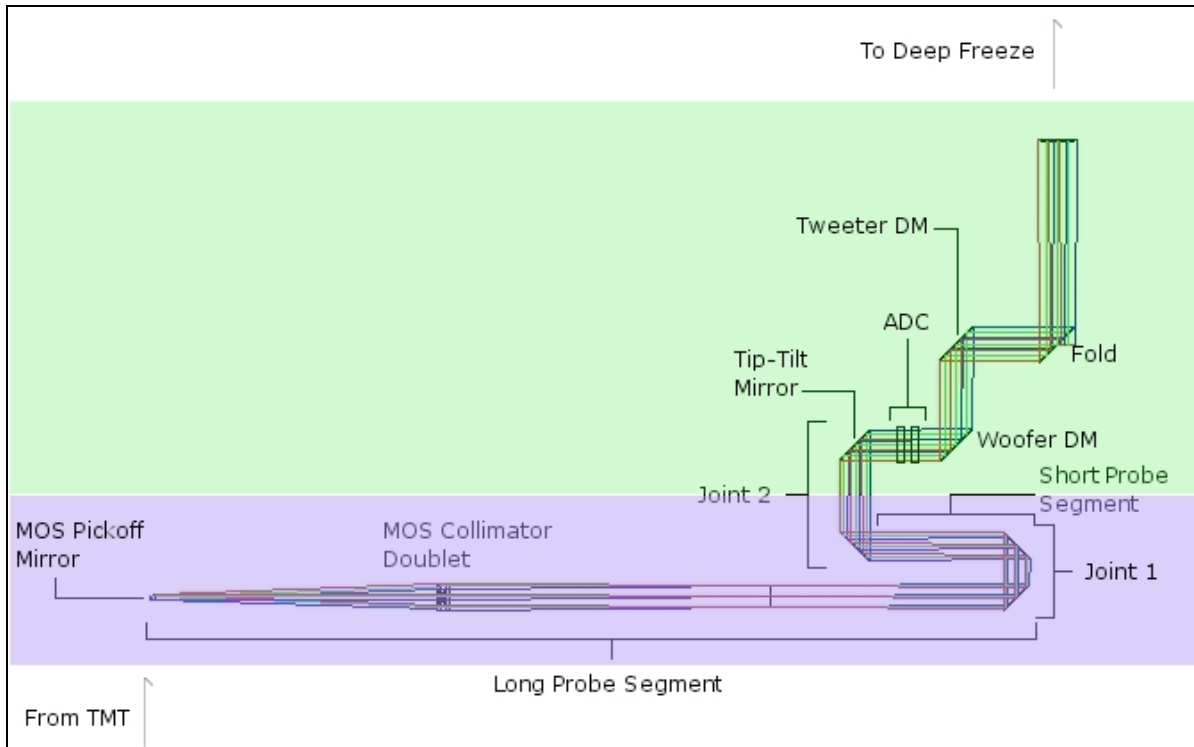


Fig. 6. IRMOs probe arm optical schematic. Blue shaded area contains moving portions of the probe, while the green shaded area contains fixed elements of the probe. The optical folds in this schematic are at right angles for illustration purposes only; the beam intersects the DMs much closer to normal incidence.

The final subsystem located in the meat locker is the truth wavefront sensor (TWFS). At the end of each MOS probe, before light enters the deep freeze, a flip mirror can be dropped in place and light from any of the MOS probes can be directed towards a central station where the TWFS will be located. This WFS can rotate to receive light from any one of the MOS probes. It will contain a high order (60x60) SH WFS feeding a low noise 1000x1000 EEV CCD201 and a 0.1 arcsecond pixel scale. The truth WFS will be used to: 1) Measure and correct non-common path differences induced by flexure between the LGS system and the MOS probes. Because the TWFS provides IRMOs information about flexure, the TWFS will have to be controlled and read out by the Real-Time Control system which is in turn capable of applying flexure corrections to the MOAO system. 2) Flatten the DMs during setup. The calibration unit's simulated source will be able to feed light to any of the scientific probe arms. This light will then pass the DMs and enter the TWFS. Thus the TWFS will be able to determine the shape of set of DMs sequentially. 3) Monitor the MOAO-corrected image quality during operation. Data from the TWFS will have to be fed by the RTC to the data management system and thence to the AO operator who will have access to the data and tools for monitoring the AO performance in real time. The TWFS data can be used to reconstruct the MOAO PSF and give immediate feedback on the ensquared energy within a given aperture being delivered to the other science probes. 4) Provide useful data relating to the quality of the MOAO tomography that will be useful when post-processing the scientific data. The data from the TWFS can be used to calibrate and check the useful information stored by the RTC which can be used to tomographically reconstruct the atmosphere and predict the PSFs for each science channel.

### 3.5 Deep Freeze Subsystems (IFUs and Spectrographs)

The deep freeze subsystem optical layout is shown in Figure 7. There are three basic optical subsystems in each deep freeze – a relay incorporating a cold pupil stop and pixel scale changer; the image slicing integral field unit, and the spectrograph itself.

Light enters the deep freeze from the top of the meatlocker at the bottom of Figure 7. The collimated beam passes through order-selecting filters held in one of 2 filter wheel mechanisms, and then encounters the MOS relay camera lenses. After passing through space-saving fold mirrors, the light enters one of three selectable relay barrels. The relays provide both a cold stop at a pupil image of the telescope secondary mirror and also provide magnification to select either the 8-mas/pix, 12-mas/pix, or 25-mas/pix plate scales for IRMOS. This light then feeds into the integral field unit (IFU, or “image slicer”), which is closely based on the FISICA image slicer (Eikenberry et al., 2004; Eikenberry et al., 2006).

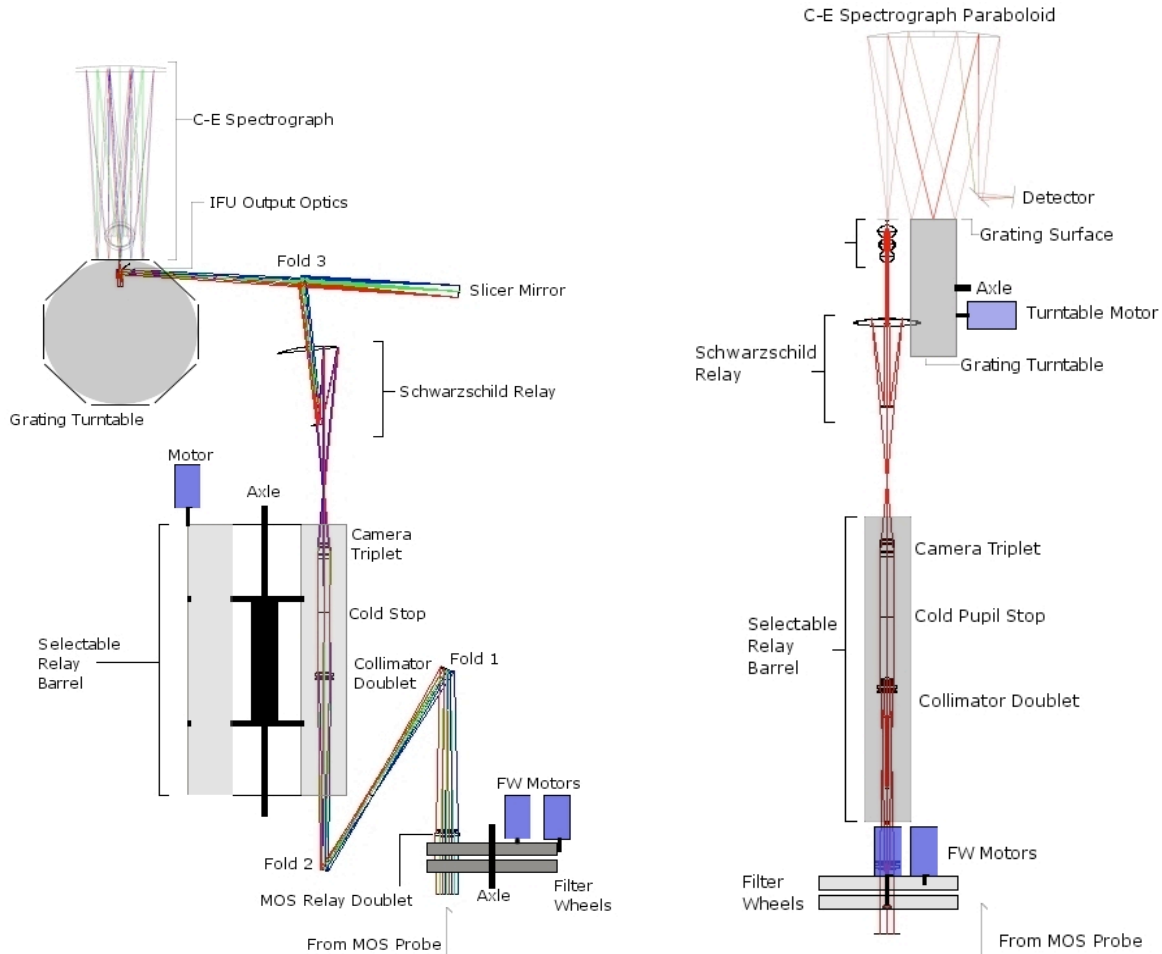


Fig. 7. IRMOS deep freeze opto-mechanical concept schematic. (Left) Front view. (Right) Side view. Only a single IFU slice and the short-focus paraboloid are shown here for clarity’s sake.

As noted above, the basic optical principle behind an image slicing IFU is to take an input 2-dimensional field-of-view, divide it into multiple “slices”, orient these slices end-to-end to create a pseudo-longslit, and then place a virtual image of this pseudo-longslit in the optical beam so that it appears to originate from the output telescope focal plane. In Figure 7, light from the scale-changer relay forms an image at a focal plane. The expanding beam encounters a 2-mirror Schwarzschild re-imaging relay, which magnifies the image and comes to a focus at the surface of the 22-element “slicer” mirror. The slicer mirror has 22 slices, each powered and independently tilted along both the “spatial” direction of the spectrograph (in order to separate the final images into a pseudo-longslit) and in the “dispersion” direction of the spectrograph (in order to separate pupil images into 2 rows of 11 each). The powered slicer mirror creates an image of the telescope exit pupil on the 22-element pupil mirror array. The pupil mirror array consists of 22 powered, offset, tilted mirrors arranged in two rows of 11 mirrors each. This 2x11 geometry was chosen in order to minimize field

angles for the IFU, and thus reduce aberrations. The pupil mirrors create another relayed de-magnified image of the telescope focal plane along a linear array of 22 field mirrors. We chose this geometry to allow the pupil mirrors to be significantly larger than the closely-spaced field mirrors, and for the field mirror array to correct telecentricity errors, and thus “offload” some tilt from the pupil mirror array. This output image plane is located at the entrance slit position of the final spectrograph optical system.

The IRMOS design uses a Cuevas-Eikenberry design – a “Cuevas” spectrograph (modified Ebert-Fastie spectrograph – see Cuevas et al. (2006)) for the fine pixel scale (8/12-mas pixels) which introduces a second selectable “Cuevas” spectrograph system for the wider-field (25-mas) pixel scales of IRMOS. The particular innovation of the Cuevas-Eikenberry design is that this second “short-focus” spectrograph maintains the same entrance slit and grating locations, and (to close approximation) detector focal location as the first “long-focus” spectrograph. This feature enables the 2 spectrographs to share the same physical volume, with no need for major motions of components (retaining mechanical simplicity and stability), and importantly, share the same gratings/mechanisms (greatly reducing complexity and optical costs). Thus, this approach retains the same advantages of the Cuevas spectrograph (good performance, simplicity of optical components, high-throughput, easy alignment) for each system, while incorporating them in a very streamlined, compact, and efficient design.

### 3.6 Calibration Unit

IRMOS will also have a separate calibration unit with both spectroscopic and adaptive optics calibration light sources. These will include multiple simulated point sources for AO calibration and testing, as well as flatfield (“dome”) and wavelength (“arc”) calibration lamps.

The authors gratefully acknowledge the support of the TMT partner institutions. They are the Association of Canadian Universities for Research in Astronomy (ACURA), the Association of Universities for Research in Astronomy (AURA), the California Institute of Technology and the University of California. This work was supported, as well, by the Canada Foundation for Innovation, the Gordon and Betty Moore Foundation, the National Optical Astronomy Observatory, which is operated by AURA under cooperative agreement with the National Science Foundation, the Ontario Ministry of Research and Innovation, and the National Research Council of Canada. The authors also acknowledge the support of the University of Florida and the Fundacion por la Preservacion del PSF.

## REFERENCES

1. D. Andersen et al., these proceedings
2. K. Hinkle et al., these proceedings
3. S. Eikenberry et al., “Systems engineering and performance modeling of the Gemini high-resolution near-infrared spectrograph (HRNIRS)”, these proceedings
4. G. Muller et al., these proceedings
5. M. Liang et al., these proceedings
6. S. Eikenberry et al., 2004, Proc. of SPIE, 5492, 1264
7. S. Eikenberry et al., “FISICA: The Florida Imager Slicer for Infrared Cosmology & Astrophysics”, these proceedings